

M^2 -Encoder: Advancing Bilingual Image-Text Understanding by Large-scale Efficient Pretraining

Qingpei Guo^{*†}, Furong Xu^{*}, Hanxiao Zhang^{*}, Wang Ren^{*},
Ziping Ma, Lin Ju, Jian Wang, Jingdong Chen, Ming Yang[†]

Ant Group

{qingpei.gqp, m.yang}@antgroup.com

Abstract

Vision-language foundation models like CLIP have revolutionized the field of artificial intelligence. Nevertheless, VLM models supporting multi-language, *e.g.*, in both Chinese and English, have lagged due to the relative scarcity of large-scale pretraining datasets. Toward this end, we introduce a comprehensive bilingual (Chinese-English) dataset BM-6B with over 6 billion image-text pairs, aimed at enhancing multimodal foundation models to well understand images in both languages. To handle such a scale of dataset, we propose a novel grouped aggregation approach for image-text contrastive loss computation, which reduces the communication overhead and GPU memory demands significantly, facilitating a 60% increase in training speed. We pretrain a series of bilingual image-text foundation models with an enhanced fine-grained understanding ability on BM-6B, the resulting models, dubbed as M^2 -Encoders (pronounced “M-Square”), set new benchmarks in both languages for multimodal retrieval and classification tasks. Notably, Our largest M^2 -Encoder-10B model has achieved top-1 accuracies of 88.5% on ImageNet and 80.7% on ImageNet-CN under a zero-shot classification setting, surpassing previously reported SoTA methods by 2.2% and 21.1%, respectively. The M^2 -Encoder series represents one of the most comprehensive bilingual image-text foundation models to date, so we are making it available to the research community for further exploration and development.¹

1 Introduction

Vision-language foundation models, such as CLIP (Radford et al., 2021a), are typically developed through contrastive learning by aligning image-text pairs on large-scale unsupervised or weakly

^{*}Co-first authors

[†]Corresponding authors

¹Github:https://github.com/alipay/Ant-Multi-Modal-Framework/tree/main/prj/M2_Encoder

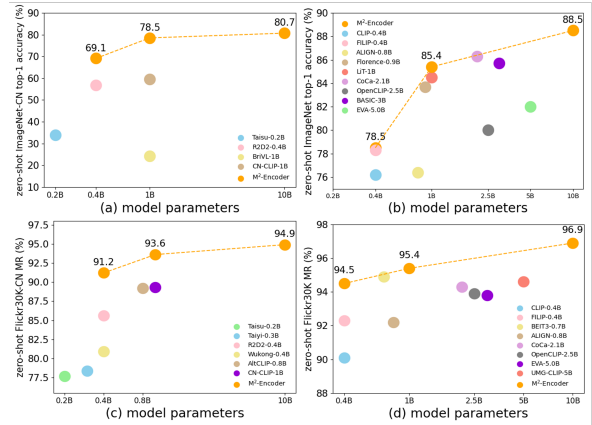


Figure 1: An overview of existing multimodal models on zero-shot classification and retrieval performance. The top-1 accuracy on (a) ImageNet-CN and (b) ImageNet. The retrieval MR on (c) Flickr30K-CN and (d) Flickr30K. Our M^2 -Encoders excel compared to models with a similar number of parameters.

supervised datasets, establishing them as fundamental components of artificial intelligence. Benefiting from their robust visual and textual representation abilities and exceptional zero-shot transferability, they are widely used in modern large-scale multimodal models, where they serve key roles in visual understanding (Ye et al., 2023; Li et al., 2023a; Gong et al., 2023; Zhu et al., 2023; Dai et al., 2023; Liu et al., 2023; Bai et al., 2023), and cross-modal alignment and generation (Ramesh et al., 2022, 2021; Rombach et al., 2022).

The performance of image-text foundational models relies heavily on large-scale image-text datasets. However, there lack of a large-scale image-text dataset in Chinese comparable to LAION2B-EN (Schuhmann et al., 2022), which might have hindered the performance of Chinese multimodal foundational models and their real-world applications. Our work aims to narrow this gap in data scales. Toward this end, we curate image-text pairs collected from public datasets and legally sourced web content, techniques such as

translation into Chinese, data cleaning to remove noise, and data augmentation to enhance variability were implemented as part of our methodology, resulting in a large-scale dataset comprising over 3 billion Chinese image-text pairs, a volume that is even larger than datasets such as LAION2B-EN. To the best of our knowledge, this collection constitutes the largest Chinese image-text dataset available to date. By integrating this corpus with English publicly available datasets(eg. LAION2B-EN, COYO-700M(Byeon et al., 2022), Datacomp-1B(Gadre et al., 2023)) and accounting for potential overlaps, we have constructed a high-quality bilingual dataset dubbed as BM-6B(BM represents bilingual multi-modality) that includes nearly 6 billion unique image-text pairs. The construction of this dataset provides a critical foundation for developing advanced bilingual multimodal models catering to both Chinese and English languages.

Training on such a massive dataset necessitates a substantial increase in computational resources. The conventional image-text contrastive (ITC) loss calculation requires gathering image-text representations from all computing nodes in a distributed system. This leads to significant communication overhead and risk of GPU memory depletion (out-of-memory errors) in large-scale training scenarios. To overcome this challenge, we design a new grouped aggregation strategy dubbed Grouped-ITC with batch accumulation(abbreviated as GBA-ITC) that evenly divides the nodes in the cluster into multiple groups. During the computation of the ITC loss, aggregation is performed within each group and coupled with batch accumulation, enabling the decoupling of the ITC loss computation from the overall batch size, leading to reduced memory requirements and enhanced scalability. This technique yields a 60% acceleration in training speed. We also adopted the "SHARING-DELINKING" training strategy proposed by the M6-10T project(Lin et al., 2021), and utilized the ReCLIP(Li et al., 2023b) strategy to expedite the convergence efficiency of training.

With the aforementioned efficient training methods, we trained a series of M^2 -Encoder models on BM-6B, with a focus on enhanced fine-grained understanding capabilities. Our M^2 -Encoders are a series of models spanning from 0.4 billion to 10 billion parameters. We conducted zero-shot evaluations of our models' performance on six bilingual cross-modal retrieval and classification test sets, in-

cluding three English test datasets: ImageNet(Deng et al., 2009), Flickr30K(Plummer et al., 2015), COCO(Chen et al., 2015), and three equivalent Chinese version test datasets, respectively: ImageNet-CN(Yang et al., 2022), Flickr30K-CN(Lan et al., 2017), and COCO-CN(Li et al., 2019). As shown in Figure 1, all of our models have achieved state-of-the-art results with comparable numbers of parameters, across multimodal retrieval and classification tasks in both Chinese and English. For fine-grained evaluation, we collect tasks requiring fine-grained perception, including fine-grained category recognition, counting, multiple object combination recognition, and relationships between objects, and established a bilingual fine-grained benchmark. Our M^2 -Encoder-10B surpass existing CLIP-based models on our fine-grained benchmark by a large margin, with an absolute improvement of 21.58% over CN-CLIP(Yang et al., 2022) for Chinese, and 15.2% over CLIP(Radford et al., 2021a) for English. Our main contributions are as follows:

- We propose BM-6B, an ultra-large dataset consisting of 6 billion image-text pairs with Chinese and English data nearly equally distributed, to mitigate the shortage of extensive Chinese image-text datasets. We verify that the BM-6B dataset is large enough to facilitate the training of bilingual image-text multimodal foundational models from scratch.
- We introduced a novel grouped aggregation strategy named GBA-ITC that leads to reduced memory requirements and enhanced scalability. This technique yields a 60% acceleration in training speed, facilitating large-scale efficient pretraining.
- We pretrain the M^2 -Encoder series models on the BM-6B dataset, placing additional emphasis on their fine-grained perception abilities. The resulting M^2 -Encoder-10B model achieves SOTA performance not only across six bilingual cross-modal retrieval and classification datasets but also excels in our constructed fine-grained perception benchmark within a zero-shot learning setup.

2 Method

2.1 M^2 -Encoder Model

Model Architecture. The availability of such a large dataset facilitates training our M^2 -Encoder

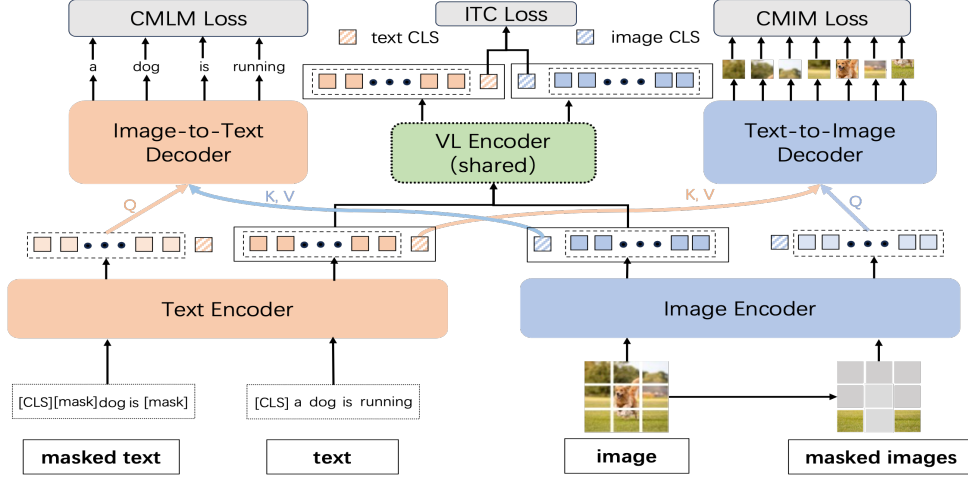


Figure 2: The pretraining tasks of the M^2 -Encoder models, including ITC, CMLM, and CMIM heads. ITC uses [CLS] token to achieve global feature alignment between image and text pair. In contrast, the CMLM and CMIM tasks employ local tokens between modalities for cross-attention to assist masked token recovery. Together, these tasks enable the M^2 -Encoder to align and integrate information across modalities at both a global and local level.

series models from scratch, allowing us to leverage cutting-edge architectures. Aiming to provide the multimodal community with highly scalable bilingual (Chinese-English) image-text foundational models, the M^2 -Encoder series of models employ the more advanced MAGNETO (Wang et al., 2023) transformer that is designed as a general-purpose architecture for multimodal and multitask applications.

Pretraining Tasks. The pretraining tasks of M^2 -Encoder is illustrated in Figure 2. For the design of proxy tasks, we referenced SyCoCa (Ma et al., 2023), which improved the CoCa pretraining tasks by introducing bidirectional interactions between images and texts. To enhance training efficiency, we opted out of the attentive masking strategy employed by SyCoCa and instead used a large proportion of random masks. Additionally, our decoder only utilized the [CLS] token from the other modality when recovering masked information. Our M^2 -Encoder has three heads: Image-Text Contrastive (ITC), Cross-modal Masked Language Modeling (CMLM), and Cross-modal Masked Image Masking (CMIM), with the latter two heads being exclusive to the training phase and not utilized during inference. For the ITC loss, we employ the [CLS] token from both image and text modalities for alignment. For the CMLM loss, we mask a large portion of the text and then use the image’s entire token set for cross-attention via an image-to-text decoder, aiding in text token prediction. Similarly, for CMIM loss—which is analogous

to CMLM—we leverage a text-to-image decoder to facilitate image recovery by inputting all text tokens and a high ratio of masked image patches. These three losses contribute to global and local cross-modal alignment, leading to improved outcomes on our constructed fine-grained benchmark.

Training Objectives. We present the mathematical formulations for each pretraining task. The ITC loss, designed to align text and image representations, is defined as:

$$\mathcal{L}_{ITC} = \frac{1}{2N} \left[\sum_i \log \left(\frac{\exp(\langle v_i^{cls}, t_i^{cls} \rangle / \tau)}{\sum_{j=1}^N \exp(\langle v_i^{cls}, t_j^{cls} \rangle / \tau)} \right) \right] + \frac{1}{2N} \left[\sum_i \log \left(\frac{\exp(\langle v_i^{cls}, t_i^{cls} \rangle / \tau)}{\sum_{j=1}^N \exp(\langle v_i^{cls}, t_j^{cls} \rangle / \tau)} \right) \right], \quad (1)$$

where v^{cls} and t^{cls} are the [CLS] tokens of image and text respectively, N is the batch size. $\langle \cdot, \cdot \rangle$ denotes the inner product, and τ is a temperature parameter that scales the logits.

The CMIM loss, inspired by Masked Autoencoders (MAE) (He et al., 2022) that reconstructs the pixels of masked image tokens, diverges from MAE by leveraging the text [CLS] token as additional context for cross-attention within the decoder. The CMIM loss function is defined as:

$$\mathcal{L}_{CMIM} = \frac{1}{M} \sum_{i=0}^P \|x_i - \hat{x}_i\|^2 \quad (2)$$

where M is the number of masked patches, P is the number of pixels in patches, x_i represents the orig-

inal pixel values, and \hat{x}_i denotes the reconstructed pixel values by the decoder.

The CMLM task is modeled as a classification problem with cross-entropy, the loss is given by:

$$\mathcal{L}_{CMLM} = -\frac{1}{N} \sum_{i=1}^N \sum_{j=1}^Q y_{ij} \log p_{ij}(x) \quad (3)$$

where N is the number of tokens in a sequence, Q is the size of the vocabulary, y_{ij} is the one-hot encoded true label for the i -th token, and $p_{ij}(x)$ is the predicted probability that the i -th token belongs to the j -th category.

The overall training objective for the M^2 -Encoders combines these losses as follows:

$$\mathcal{L}_{overall} = \mathcal{L}_{ITC} + \alpha \mathcal{L}_{CMIM} + \beta \mathcal{L}_{CMLM} \quad (4)$$

where α and β are hyperparameters that balance the relative importance of the CMIM and CMLM tasks in the overall training objective.

2.2 Training Dataset

Data Sources. A significant contributor to the outstanding performance of the M^2 -Encoder models is our construction of the large-scale BM-6B dataset. This dataset comprises approximately 6 billion bilingual image-text pairs, with each language constituting half of the dataset. The majority of these pairs were sourced from publicly available datasets. The English data within the BM-6B dataset are derived from Laion-EN (Schuhmann et al., 2022), COYO-700M (Byeon et al., 2022), Datacomp-1B (Gadre et al., 2023), and Generated Datacomp’s Large Pool (Nguyen et al., 2023), while the Chinese portion is primarily sourced from Laion-CN, Wukong (Carver et al., 2020), Taisu (Liu et al., 2022), and Zero (Xie et al., 2023). Additionally, to enhance the diversity of the training dataset, we incorporated 680 million Chinese in-house data samples and translated the Laion-EN dataset into Chinese. The detailed distribution of the training data is presented in Appendix C.

Data Cleaning. Besides the quantity, the quality of data is crucial for the effectiveness of the model. To improve the quality of the BM-6B dataset, we developed a data cleaning pipeline. We first remove samples if they satisfy any of the following conditions: the text length is less than 5 characters, which typically indicates insufficient descriptive content, or the image aspect ratio exceeds 3, suggesting distorted or extreme image dimensions. For the

samples that remain, we calculate the image-text semantic similarity with CLIP, retaining samples of high correspondence with a semantic score exceeding a threshold of 0.25. For samples with similarity scores below this specified threshold, we apply data augmentation techniques such as paraphrasing to revise captions, thereby improving alignment between images and texts and enhancing the overall utilization of the data.

Data Augmentation. Building upon the findings of Nguyen et al. (2023) (Nguyen et al., 2023) that synthetic captions can be used to improve multi-modal dataset quality, we propose a method to generate captions with improved relevance to the associated images in our BM-6B dataset. To achieve this, we aim to enhance the contextual alignment and coherence between raw and synthetic captions by training a rewritten model. As a first step, we utilize the BLIP2 (Li et al., 2023a) model to generate synthetic captions for each image. Then, annotators are provided with guidelines to revise the original captions by considering the image content and the BLIP2-generated captions, and they are encouraged to preserve terms from the raw captions where appropriate, ensuring that these terms do not introduce misleading or incorrect details that are not evident in the image. Subsequently, we adapt the BLIP2 model into a rewritten model that is fine-tuned to take the image and original captions as input, and to produce the refined annotations as output. Once the fine-tuning process is complete, the resulting model is ready to generate improved captions for image-text pairs with low CLIP scores.

Table 12 displays the quantities of data remaining from each source dataset after the application of data cleaning and data augmentation procedures.

2.3 Training Infrastructure

Our training cluster consists of up to 32 NVIDIA DGX nodes, each equipped with 8 Ampere A100-SXM3-80G GPUs. In general, the application of training strategies such as PyTorch’s Fully Sharded Data Parallel (FSDP)² for parameter sharding is feasible for large-scale model training, since it demonstrates horizontal scalability of training resources. However, our model involves the computation of ITC loss. Conventional computation of ITC loss, as illustrated in Figure 3 (a), necessitates the collection of image-text representations from all GPUs within the distributed system at each training

²<https://pytorch.org/docs/1.11/fsdp.html>

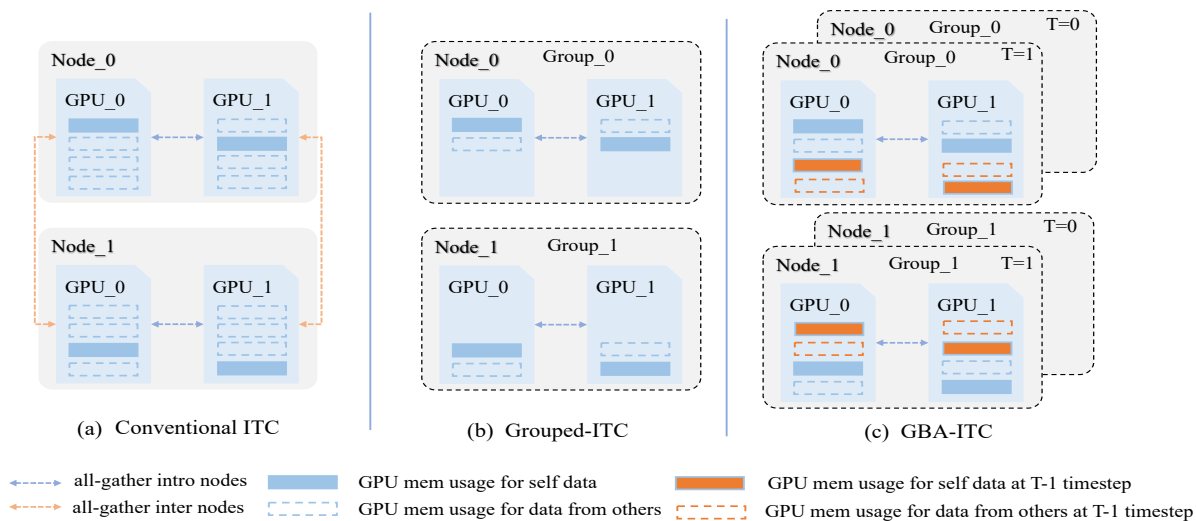


Figure 3: Illustration of conventional ITC, Grouped-ITC and GBA-ITC’s data collection process before loss calculation with 2 nodes. GBA-ITC demonstrates the least communication overload.

step. This requirement engenders two significant challenges: 1. Frequent invocation of the all-gather operation across all nodes during training can result in a communication bandwidth bottleneck, thereby impeding efficient scaling in large-scale training scenarios. 2. As training scales, there is a linear increase in the volume of data aggregated on each GPU, leading to elevated peak memory usage and a higher risk of GPU memory depletion, especially with larger overall batch sizes.

We propose a new grouped aggregation strategy dubbed Grouped-ITC with batch accumulation (abbreviated as GBA-ITC) to address these issues. The idea of Grouped-ITC is inspired by FSDP so that one can have multiple FSDP units, with the all-gather operation being executed only within each FSDP unit, thus minimizing unnecessary data movement and leading to reduced communication overhead. Our proposed Grouped-ITC inherits this concept by evenly partitioning the cluster nodes into multiple groups and then performing all-gather within each group during the ITC loss calculation. We illustrate this process with a 2 nodes example shown in Figure 3(b), after dividing all nodes into two groups, by implementing Grouped-ITC, the peak GPU memory requirement (2 units per GPU) is reduced by half compared to conventional ITC (4 units per GPU), as well as reducing the all-gather communication overhead. Grouped-ITC’s reduction in peak GPU memory usage enables accumulating training samples through multiple for-

ward passes with a single gradient backpropagation step. By combining Grouped-ITC with batch accumulation, we achieve increased batch sizes and enhanced training efficiency. This method is designated as GBA-ITC and is depicted in Figure 3(c).

3 Experiments

We train M^2 -Encoder models of various sizes and evaluate them as follows. Detailed model configurations and training settings are provided in Appendix A.

3.1 Evaluation Setting

Coarse-grained Understanding. To evaluate our image-text coarse understanding capabilities, we utilize several open Chinese and English retrieval and classification datasets. For English understanding, we assess zero-shot image-text retrieval capabilities on the Flickr30K (Plummer et al., 2015) and COCO (Chen et al., 2015) datasets, and zero-shot image classification on ImageNet (Deng et al., 2009), using the experimental setup described in CoCa (Yu et al., 2022). For Chinese understanding, in line with evaluation method used by CN-CLIP (Yang et al., 2022), we employ Flickr30K-CN and COCO-CN to test zero-shot image-text retrieval, and ImageNet-CN to evaluate zero-shot image classification capabilities.

Fine-grained Understanding. To evaluate fine-grained capabilities-including recognition of fine-grained categories, counting abilities, recognition

of multiple object combinations, and understanding of relationships between objects—we constructed a fine-grained benchmark comprising seven diverse datasets. For a detailed description of the datasets included in this benchmark, readers are referred to Appendix B.

Evaluation Metrics. For tasks such as image-text retrieval and fine-grained retrieval, unless otherwise stated, we use the Mean Recall at top-1, top-5, and top-10 ranks for both text-to-image and image-to-text retrieval as our primary evaluation metrics. For the image classification task, we report the top-1 accuracy, which refers to the top-1 recall in a zero-shot setting.

Method	Accuracy
CLIP-0.4B (Radford et al., 2021b)	76.2
ALIGN-0.8B (Jia et al., 2021)	76.4
FILIP-0.4B (Yao et al., 2021)	78.3
Florence-0.9B (Yuan et al., 2021)	83.7
LiT-1B (Zhai et al., 2022a)	84.5
BASIC-0.4B (Pham et al., 2021)	81.5
BASIC-3B (Pham et al., 2021)	85.7
OpenCLIP-1.3B (Cherti et al., 2023)	78.5
OpenCLIP-2.5B (Cherti et al., 2023)	80.0
CoCa-0.4B (Yu et al., 2022)	82.6
CoCa-0.8B (Yu et al., 2022)	84.8
CoCa-2.1B (Yu et al., 2022)	<u>86.3</u>
EVA-1.1B (Sun et al., 2023)	78.5
EVA-5.0B (Sun et al., 2023)	82.0
M^2 -Encoder-0.4B	78.5
M^2 -Encoder-1B	85.4
M^2 -Encoder-10B	88.5

Table 1: Zero-shot image classification evaluation results on ImageNet. Metrics denoted by an underscore represent the previous SOTA, while metrics presented in bold indicate surpassing previous SOTA.

3.2 Main Results

Image Classification. The zero-shot image classification results for English and Chinese benchmarks are shown in Table 1 and Table 2, respectively. In the English benchmark, our M^2 -Encoder-0.4B and M^2 -Encoder-1B outperform other methods with a similar number of parameters, while the M^2 -Encoder-10B achieves SOTA results on ImageNet. For Chinese image classification, as detailed in Table 2, our M^2 -Encoders surpass all existing methods. These experimental results underscore our method’s effectiveness in both English and Chinese image classification tasks.

Method	Accuracy
BriVL-1B (Huo et al., 2021)	24.3
Taisu-0.2B (Liu et al., 2022)	34.0
Wukong (Gu et al., 2022)	56.9
CN-CLIP-0.2B (Yang et al., 2022)	48.3
CN-CLIP-1B (Yang et al., 2022)	<u>59.6</u>
M^2 -Encoder-0.4B	69.1
M^2 -Encoder-1B	78.5
M^2 -Encoder-10B	80.7

Table 2: Zero-shot image classification evaluation results on ImageNet-CN. Metrics denoted by an underscore represent the previous SOTA, while metrics presented in bold indicate surpassing previous SOTA.

Image-Text Retrieval. The zero-shot retrieval results on English and Chinese benchmarks are shown in Table 4 and Table 5, respectively. From Table 4, we can observe that our M^2 -Encoders exhibit superior performance in English image-text retrieval tasks. Specifically, M^2 -Encoder-0.4B surpasses models with an equivalent number of parameters. M^2 -Encoder-1B outperforms all existing methods, including those with larger parameter sizes such as OpenCLIP-2.5B, CoCa-2.1B and EVA-5.0B. Additionally, our M^2 -Encoder-10B achieves the best results, with a gain in MR of 2.0% on Flickr30K and 1.2% on COCO. For Chinese image-text retrieval, the results are presented in Table 5. Our M^2 -Encoders outperform all other methods across a range of model parameters on both Flickr30K-CN and COCO-CN.

Fine-grained Retrieval. Our M^2 -Encoders introduce token-level local alignment to enhance fine-grained capabilities. Table 3 presents the fine-grained retrieval results on seven datasets, encompassing both Chinese and English languages. To highlight the fine-grained advantages of the M^2 -Encoders, we used the open-source models CN-CLIP-1B (Yang et al., 2022) and CLIP (Radford et al., 2021b) as baselines for Chinese and English retrieval, respectively. Our method exhibits a superior fine-grained retrieval performance, with even the smallest variant, M^2 -Encoder-0.4B, outstripping the baseline models on the majority of the fine-grained datasets. This affirms the efficacy of our method in fine-grained understanding and modeling.

Method(CN/EN)	CUB-200-2011	Stanford-Dogs	CARS196	COCO-MCC	COCO-COUNT	VG-POS	HOI-POS	Overall MR
CLIP-0.4B (Radford et al., 2021b)	-/81.56	-/75.71	-/87.98	-/22.42	-/17.87	-/13.33	-/63.31	-/51.74
CN-CLIP-1B (Yang et al., 2022)	24.16/-	48.81/-	83.58/-	20.6/-	14.54/-	9.96/-	68.51/-	<u>38.59/-</u>
M^2 -Encoder-0.4B	73.72/57.22	85.19/84.66	94.14/91.54	41.27/38.54	25.48/24.47	23.74/21.04	75.44/70.94	59.85/55.49
M^2 -Encoder-1B	79.48/68.48	91.04/91.95	94.14/94.21	48.24/46.71	29.18/31.27	27.39/25.77	81.21/79.10	64.38/62.50
M^2 -Encoder-10B	89.56/86.62	92.5/91.97	97.41/97.80	55.13/50.91	36.04/33.77	32.78/26.96	84.45/80.57	69.70/66.94

Table 3: Zero-shot fine-grained retrieval evaluation results on 7 Chinese and English datasets. Metrics denoted by an underscore represent the previous SOTA, while metrics presented in bold indicate surpassing previous SOTA.

Method	Flickr30K								MSCOCO							
	Text → Image				Image → Text				Text → Image				Image → Text			
	R@1	R@5	R@10	MR	R@1	R@5	R@10	MR	R@1	R@5	R@10	MR	R@1	R@5	R@10	MR
CLIP-0.4B (Radford et al., 2021b)	68.7	90.6	95.2	88.0	98.7	99.4	90.1	37.8	62.4	72.2	58.4	81.5	88.1	66.7		
ALIGN-0.8B (Jia et al., 2021)	75.7	93.8	96.8	88.6	98.7	99.7	92.2	45.6	69.8	78.6	58.6	83.0	89.7	70.9		
FLAVA-0.3B (Singh et al., 2022)	65.2	89.4	-	67.7	94.0	-	-	38.4	67.5	-	42.7	76.8	-	-		
FILIP-0.4B (Yao et al., 2021)	75.0	93.4	96.3	89.8	99.2	99.8	92.3	45.9	70.6	79.3	61.3	84.3	90.4	72.0		
Florence-0.9B (Yuan et al., 2021)	76.7	93.6	-	90.9	99.1	-	-	47.2	71.4	-	64.7	85.9	-	-		
BEIT3-0.7B (Wang et al., 2022)	81.5	95.6	97.8	94.9	99.9	100	<u>94.9</u>	-	-	-	-	-	-	-		
OpenCLIP-1.3B (Cherti et al., 2023)	77.7	94.1	96.9	91.4	99.2	99.6	93.1	48.8	73.3	81.5	66.4	86.0	91.8	74.6		
OpenCLIP-2.5B (Cherti et al., 2023)	79.5	95.0	97.1	92.9	99.3	99.8	93.9	51.4	74.9	83.0	67.3	86.9	92.6	76.0		
CoCa-0.4B (Yu et al., 2022)	76.8	93.7	96.8	89.8	98.8	99.8	92.6	47.5	72.4	80.9	63.8	84.7	90.7	73.3		
CoCa-0.8B (Yu et al., 2022)	79.0	95.1	97.4	91.4	99.2	99.9	93.7	50.1	73.8	81.8	65.4	85.6	91.4	74.7		
CoCa-2.1B (Yu et al., 2022)	80.4	95.7	97.7	92.5	99.5	99.9	94.3	51.2	74.2	82.0	66.3	86.2	91.8	75.3		
EVA-1.1B (Sun et al., 2023)	72.6	91.6	95.1	88.3	98.3	99.3	90.9	44.1	68.5	77.3	61.8	83.3	90.0	70.8		
EVA-5.0B (Sun et al., 2023)	78.8	94.2	96.8	93.9	99.4	99.8	93.8	51.1	75.0	82.7	68.8	87.8	92.8	76.4		
ERNIE-ViL 2.0 (Shan et al., 2022)	77.4	93.8	96.4	91.2	99.1	99.8	92.9	46.0	71.4	80.4	63.1	85.7	91.4	73.0		
AltCLIP-0.8B (Chen et al., 2022)	72.5	91.6	95.4	86.0	98.0	99.1	90.4	42.9	68.0	77.4	58.6	80.6	87.8	69.2		
UMG-CLIP-0.4B (Shi et al., 2024)	83.1	96.0	98.1	93.4	99.5	99.9	95.0	54.6	78.5	86.1	68.9	89.0	94.1	78.5		
UMG-CLIP-5B (Shi et al., 2024)	81.2	95.7	97.7	93.1	99.7	99.9	94.6	57.5	80.4	87.3	71.7	89.8	94.3	<u>80.2</u>		
M^2 -Encoder-0.4B	87.2	97.9	99.4	85.2	98.2	99.4	94.5	49.0	76.1	85.0	62.5	86.4	92.7	75.2		
M^2 -Encoder-1B	88.8	98.9	99.5	87.6	98.3	99.4	95.4	51.5	76.8	85.0	67.4	87.7	93.2	76.9		
M^2 -Encoder-10B	92.2	99.5	99.7	91.2	99.2	99.6	96.9	56.5	81.6	88.8	72.8	92.3	96.3	81.4		

Table 4: Zero-shot image-text retrieval evaluation results on Flickr30K and MSCOCO dataset. Metrics denoted by an underscore represent the previous SOTA, while metrics presented in bold indicate surpassing previous SOTA.

3.3 Ablation Study

Benefits of Large Training Sets. We studied the impact of the size of our BM-6B pretraining dataset. For this experiment, we take subsets of approximately 33% and 67% from our BM-6B dataset and pre-train the M^2 -Encoder-1B model using the same setup as above. As shown in Table 7, we can observe that the performance of M^2 -Encoder-1B grows monotonically as the usage of image-text pairs from BM-6B increases, which suggests that our M^2 -Encoders may benefit from even more pre-training data.

Effectiveness of Pretraining Tasks. The enhanced fine-grained understanding ability makes our M^2 -Encoder series models distinct from existing ones. To validate the effectiveness of our pretraining tasks in this domain, we trained an M^2 -Encoder-1B variant (dubbed ITC-only) employing only ITC loss employed as a baseline for comparative analysis. The results are demonstrated in Table 8. With the aid of our fine-grained pertaining loss, our M^2 -Encoder-1B outperforms its ITC-only

counterpart by a large margin on tasks requiring detailed perception, illustrating the effectiveness of our pretraining approach on fine-grained understanding.

Effectiveness of GBA-ITC. To verify the effectiveness of GBA-ITC, comparative experiments (detailed in Table 6) were conducted on both performance and effectiveness using 4 DGX nodes (8GPUs per node). Results are shown in Figure 4. It can be observed that under the same global batch size setting, both Grouped-ITC and GBA-ITC exhibit convergence behavior analogous to that of the conventional ITC with regard to loss metrics. The observed minor fluctuations in loss metrics may be attributed to batch accumulation operations in GBA-ITC, which result in less frequent optimization and parameter updates over an equivalent number of iterations. Regarding throughput, the Grouped-ITC method, which performs aggregation within each group, incurs lower communication overhead compared to the conventional ITC baseline. This efficiency translates to a throughput improvement factor of 1.07X. Additionally, GBA-

Method	Flickr30K-CN							COCO-CN						
	Text → Image			Image → Text				Text → Image			Image → Text			
	R@1	R@5	R@10	R@1	R@5	R@10	MR	R@1	R@5	R@10	R@1	R@5	R@10	MR
BriVL-1B (Huo et al., 2021)	10.3	27.5	37.9	17.7	42.3	54.3	31.7	14.8	39.0	54.2	17.1	41.7	57.5	37.4
Taiyi-0.3B (Luo et al., 2023)	53.7	79.8	86.6	63.8	90.5	95.9	78.4	-	-	-	-	-	-	-
Wukong-0.4B (Gu et al., 2022)	51.7	78.9	86.3	76.1	94.8	97.5	80.9	53.4	80.2	90.1	55.2	81.0	90.6	75.1
Taisu-0.2B (Liu et al., 2022)	49.9	78.9	87.0	65.6	90.1	94.9	77.7	53.6	83.7	92.4	52.5	81.5	91.4	75.9
CN-CLIP-0.2B (Yang et al., 2022)	62.7	86.9	92.8	74.6	93.5	97.1	84.6	57.0	84.1	93.6	62.2	86.6	94.9	79.7
CN-CLIP-1B (Yang et al., 2022)	71.2	91.4	95.5	81.6	97.5	98.8	<u>89.3</u>	69.2	89.9	96.1	63.0	86.6	92.9	83.0
R2D2-0.4B (Xie et al., 2022)	60.9	86.8	92.7	77.6	96.7	98.9	85.6	56.4	85.0	93.1	63.3	89.3	95.7	80.5
AltCLIP-0.8B (Chen et al., 2022)	69.8	89.9	94.7	84.8	97.4	98.8	89.2	61.3	86.0	93.2	77.8	94.4	97.5	85.0
ERNIE-ViL 2.0 (Shan et al., 2022)	-	-	-	-	-	-	-	69.6	91.2	96.9	69.1	92.9	97.1	<u>86.1</u>
M^2 -Encoder-0.4B	72.5	92.4	96.4	87.9	98.4	99.4	91.2	72.5	93.7	97.7	71.0	93.7	97.9	87.8
M^2 -Encoder-1B	78.6	94.8	97.6	91.5	99.3	99.7	93.6	75.9	95.1	98.3	74.6	94.2	98.0	89.3
M^2 -Encoder-10B	81.5	96.2	98.5	93.8	99.7	99.9	94.9	78.7	96.0	98.7	80.9	96.5	99.1	91.7

Table 5: Zero-shot image-text retrieval evaluation results on Flickr30K-CN and COCO-CN dataset. Metrics denoted by an underscore represent the previous SOTA, while metrics presented in bold indicate surpassing previous SOTA.

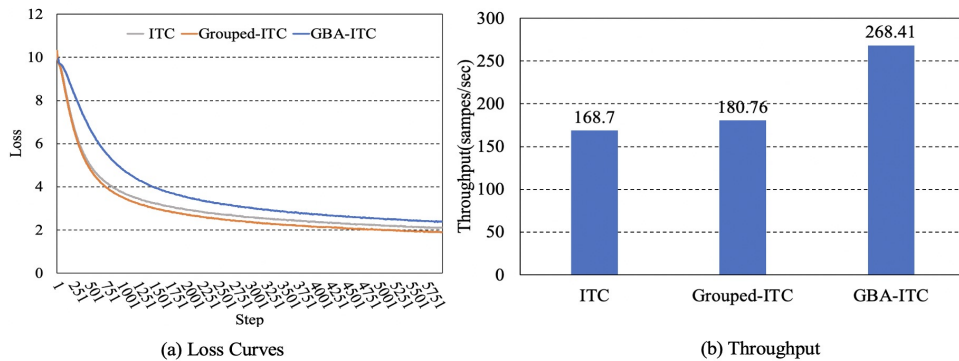


Figure 4: Comparison of loss curves and throughput among ITC, Grouped-ITC and GBA-ITC.

Setting	Batch-size per GPU	Group-size (#GPUs)	Batch-Acc steps
ITC	512	32	1
Grouped-ITC	1024	16	1
GBA-ITC	1024	8	2

Table 6: Experimental configuration for conventional ITC, Grouped-ITC and GBA-ITC. All ITC losses calculation involve an equal number of samples. Group size means the number of GPUs involved in data aggregation for loss computation, and Batch-Acc steps represents for batch accumulation steps for each GPU.

ITC leverages smaller group sizes coupled with batch accumulation to effectively diminish communication costs, culminating in a further throughput enhancement of 1.59X. The group size of GBA-ITC can be flexibly configured, enabling the decoupling of the ITC loss computation from the overall batch size. In our experiment with same batch size per GPU, reducing the group size from 32 to 16 resulted in peak memory usage being reduced by approximately half(from 50.42GB to 27.46GB). These findings indicate that GBA-ITC is effective in mitigating the challenges of communication bottlenecks and high peak memory usage, thus fa-

Method	Flickr30K-CN			COCO-CN		
	T2I-MR	I2T-MR	MR	T2I-MR	I2T-MR	MR
M^2 -Encoder-1B(33%)	85.6	94.6	90.1	83.0	85.5	84.3
M^2 -Encoder-1B(67%)	89.0	96.6	92.8	88.9	89.6	89.2
M^2 -Encoder-1B(100%)	90.3	96.8	93.6	89.8	88.9	89.3

Table 7: Evaluation results for pertaining M^2 -Encoder-1B with different percentage of the proposed BM-6B dataset.

cilitating efficient scaling in large-scale training scenarios.

4 Related Work

Recent advancements in adapting VLMs for Chinese language understanding include CN-CLIP(Yang et al., 2022) and AltCLIP(Chen et al., 2022). CN-CLIP enhances CLIP(Radford et al., 2021a) with Chinese language support by utilizing locked-image tuning(Zhai et al., 2022b) to keep the CLIP visual Encoder constant while aligning it with a Chinese text encoder in the first stage, followed by contrastive fine-tuning using a dataset of 200 million Chinese image-text pairs in the second stage. Meanwhile, AltCLIP extends CLIP with Chinese support by aligning the CLIP text

Method(CN)	CUB-200-2011	Stanford-Dogs	CARS196	COCO-MCC	COCO-COUNT	VG-POS	HOI-POS	Overall MR
M^2 -Encoder-1B w/ ITC-only	68.52	86.93	90.93	40.44	25.26	22.62	76.28	58.71
M^2 -Encoder-1B	79.48	91.04	94.14	48.24	29.18	27.39	81.21	64.38

Table 8: Ablation on the effectiveness of pretraining tasks for fine-grained understanding.

encoder with a multilingual text encoder using a teacher-learning approach. Our approach differs from the methods mentioned above in three key aspects: Firstly, unlike CN-CLIP and AltCLIP, which build upon the existing CLIP model, our bilingual M^2 -Encoders are developed without relying on any pre-existing pretrained models, directly trained from scratch using the massive bilingual BM-6B dataset. Secondly, these CLIP-based models tend to underperform on tasks that require detailed perception, since they rely on using only the ITC task for cross-modal alignment. Our M^2 -Encoders are trained with enhanced fine-grained understanding capability. Thirdly, CN-CLIP and AltCLIP are limited to a maximum model size of 1B parameters, potentially constraining their ability to capture intricate patterns. Our scalable model architecture and the BM-6B dataset have enabled us to train a model with up to 10 billion parameters. This has resulted in setting new state-of-the-art benchmarks in both Chinese and English multimodal tasks and is known to be the largest-scale bilingual contrastive-based vision-language model to date.

5 Conclusion

In this work, we propose M^2 -Encoders, a series of bilingual vision-language foundation models with multiple sizes ranging from 0.4B to 10B parameters that facilitate both coarse and fine-grained understanding. To adequately train the M^2 -Encoders from scratch, we construct the BM-6B, an ultra-large bilingual pretraining dataset comprising 6 billion image-text pairs with Chinese and English data nearly equally distributed, addressing the need for diverse and extensive bilingual datasets. To facilitate efficient scaling in large-scale training, we introduce the GBA-ITC method for reduced communication overhead and high peak memory usage. Our comprehensive evaluation shows that M^2 -Encoders, particularly the 10B variant, set new benchmarks in both languages for multimodal retrieval and classification tasks. Furthermore, we underscore that M^2 -Encoders can also achieve competitive performance in zero-shot fine-grained retrieval across 7 diverse datasets.

References

- Jinze Bai, Shuai Bai, Shusheng Yang, Shijie Wang, Sinan Tan, Peng Wang, Junyang Lin, Chang Zhou, and Jingren Zhou. 2023. [Qwen-vl: A frontier large vision-language model with versatile abilities](#).
- Minwoo Byeon, Beomhee Park, Haecheon Kim, Sungjun Lee, Woonhyuk Baek, and Saehoon Kim. 2022. Coyo-700m: Image-text pair dataset. <https://github.com/kakaobrain/coyo-dataset>.
- Benjamin Carver, Jingyuan Zhang, Ao Wang, Ali Anwar, Panruo Wu, and Yue Cheng. 2020. Wukong: A scalable and locality-enhanced framework for serverless parallel computing. In *Proceedings of the 11th ACM symposium on cloud computing*, pages 1–15.
- Yu-Wei Chao, Zhan Wang, Yugeng He, Jiaxuan Wang, and Jia Deng. 2015. Hico: A benchmark for recognizing human-object interactions in images. In *Proceedings of the IEEE international conference on computer vision*, pages 1017–1025.
- Xinlei Chen, Hao Fang, Tsung-Yi Lin, Ramakrishna Vedantam, Saurabh Gupta, Piotr Dollár, and C Lawrence Zitnick. 2015. Microsoft coco captions: Data collection and evaluation server. *arXiv preprint arXiv:1504.00325*.
- Zhongzhi Chen, Guang Liu, Bo-Wen Zhang, Fulong Ye, Qinghong Yang, and Ledell Wu. 2022. Altclip: Altering the language encoder in clip for extended language capabilities. *arXiv preprint arXiv:2211.06679*.
- Mehdi Cherti, Romain Beaumont, Ross Wightman, Mitchell Wortsman, Gabriel Ilharco, Cade Gordon, Christoph Schuhmann, Ludwig Schmidt, and Jenia Jitsev. 2023. Reproducible scaling laws for contrastive language-image learning. In *Proceedings of the IEEE/CVF Conference on Computer Vision and Pattern Recognition*, pages 2818–2829.
- Wenliang Dai, Junnan Li, Dongxu Li, Anthony Meng Huat Tiong, Junqi Zhao, Weisheng Wang, Boyang Li, Pascale Fung, and Steven Hoi. 2023. [Instructblip: Towards general-purpose vision-language models with instruction tuning](#).
- Jia Deng, Wei Dong, Richard Socher, Li-Jia Li, Kai Li, and Li Fei-Fei. 2009. Imagenet: A large-scale hierarchical image database. In *2009 IEEE conference on computer vision and pattern recognition*, pages 248–255. Ieee.
- Samir Yitzhak Gadre, Gabriel Ilharco, Alex Fang, Jonathan Hayase, Georgios Smyrnis, Thao Nguyen, Ryan Marten, Mitchell Wortsman, Dhruva Ghosh, Jieyu Zhang, et al. 2023. [Datacomp: In search of the next generation of multimodal datasets](#).

- Tao Gong, Chengqi Lyu, Shilong Zhang, Yudong Wang, Miao Zheng, Qian Zhao, Kuikun Liu, Wenwei Zhang, Ping Luo, and Kai Chen. 2023. [Multimodal-gpt: A vision and language model for dialogue with humans](#).
- Jiayi Gu, Xiaojun Meng, Guansong Lu, Lu Hou, Niu Minzhe, Xiaodan Liang, Lewei Yao, Runhui Huang, Wei Zhang, Xin Jiang, et al. 2022. Wukong: A 100 million large-scale chinese cross-modal pre-training benchmark. *Advances in Neural Information Processing Systems*, 35:26418–26431.
- Kaiming He, Xinlei Chen, Saining Xie, Yanghao Li, Piotr Dollár, and Ross Girshick. 2022. Masked autoencoders are scalable vision learners. In *Proceedings of the IEEE/CVF conference on computer vision and pattern recognition*, pages 16000–16009.
- Yuqi Huo, Manli Zhang, Guangzhen Liu, Haoyu Lu, Yizhao Gao, Guoxing Yang, Jingyuan Wen, Heng Zhang, Baogui Xu, Weihao Zheng, et al. 2021. Wenlan: Bridging vision and language by large-scale multi-modal pre-training. *arXiv preprint arXiv:2103.06561*.
- Chao Jia, Yinfei Yang, Ye Xia, Yi-Ting Chen, Zarana Parekh, Hieu Pham, Quoc Le, Yun-Hsuan Sung, Zhen Li, and Tom Duerig. 2021. Scaling up visual and vision-language representation learning with noisy text supervision. In *International conference on machine learning*, pages 4904–4916. PMLR.
- Aditya Khosla, Nityananda Jayadevaprakash, Bangpeng Yao, and Fei-Fei Li. 2011. Novel dataset for fine-grained image categorization: Stanford dogs. In *Proc. CVPR workshop on fine-grained visual categorization (FGVC)*, volume 2. Citeseer.
- Jonathan Krause, Michael Stark, Jia Deng, and Li Fei-Fei. 2013. 3d object representations for fine-grained categorization. In *Proceedings of the IEEE international conference on computer vision workshops*, pages 554–561.
- Ranjay Krishna, Yuke Zhu, Oliver Groth, Justin Johnson, Kenji Hata, Joshua Kravitz, Stephanie Chen, Yannis Kalantidis, Li-Jia Li, David A Shamma, et al. 2017. Visual genome: Connecting language and vision using crowdsourced dense image annotations. *International journal of computer vision*, 123:32–73.
- Weiyu Lan, Xirong Li, and Jianfeng Dong. 2017. Fluency-guided cross-lingual image captioning. In *Proceedings of the 25th ACM international conference on Multimedia*, pages 1549–1557.
- Junnan Li, Dongxu Li, Silvio Savarese, and Steven Hoi. 2023a. [Blip-2: Bootstrapping language-image pre-training with frozen image encoders and large language models](#).
- Runze Li, Dahun Kim, Bir Bhanu, and Weicheng Kuo. 2023b. [Reclip: Resource-efficient clip by training with small images](#).
- Xirong Li, Chaoxi Xu, Xiaoxu Wang, Weiyu Lan, Zhengxiong Jia, Gang Yang, and Jieping Xu. 2019. Coco-cn for cross-lingual image tagging, captioning, and retrieval. *IEEE Transactions on Multimedia*, 21(9):2347–2360.
- Junyang Lin, An Yang, Jinze Bai, Chang Zhou, Le Jiang, Xianyan Jia, Ang Wang, Jie Zhang, Yong Li, Wei Lin, et al. 2021. [M6-10t: A sharing-delinking paradigm for efficient multi-trillion parameter pretraining](#).
- Haotian Liu, Chunyuan Li, Qingyang Wu, and Yong Jae Lee. 2023. [Visual instruction tuning](#).
- Yulong Liu, Guibo Zhu, Bin Zhu, Qi Song, Guojing Ge, Haoran Chen, GuanHui Qiao, Ru Peng, Lingxiang Wu, and Jinqiao Wang. 2022. Taisu: A 166m large-scale high-quality dataset for chinese vision-language pre-training. *Advances in Neural Information Processing Systems*, 35:16705–16717.
- Ling Luo, Jinzhong Ning, Yingwen Zhao, Zhijun Wang, Zeyuan Ding, Peng Chen, Weiru Fu, Qinyu Han, Guangtao Xu, Yunzhi Qiu, et al. 2023. Taiyi: A bilingual fine-tuned large language model for diverse biomedical tasks. *arXiv preprint arXiv:2311.11608*.
- Ziping Ma, Furong Xu, Liu Jian, Yang Ming, and Guo Qingpei. 2023. [Sycoca: Symmetrizing contrastive captioners with attentive masking for multimodal alignment](#).
- Thao Nguyen, Samir Yitzhak Gadre, Gabriel Ilharco, Sewoong Oh, and Ludwig Schmidt. 2023. [Improving multimodal datasets with image captioning](#).
- Hieu Pham, Zihang Dai, Golnaz Ghiasi, Kenji Kawaguchi, Hanxiao Liu, Adams Wei Yu, Jiahui Yu, Yi-Ting Chen, Minh-Thang Luong, Yonghui Wu, et al. 2021. Combined scaling for open-vocabulary image classification. *arXiv e-prints*, pages arXiv–2111.
- Bryan A Plummer, Liwei Wang, Chris M Cervantes, Juan C Caicedo, Julia Hockenmaier, and Svetlana Lazebnik. 2015. Flickr30k entities: Collecting region-to-phrase correspondences for richer image-to-sentence models. In *Proceedings of the IEEE international conference on computer vision*, pages 2641–2649.
- Alec Radford, Jong Wook Kim, Chris Hallacy, Aditya Ramesh, Gabriel Goh, Sandhini Agarwal, Girish Sastry, Amanda Askell, Pamela Mishkin, Jack Clark, et al. 2021a. [Learning transferable visual models from natural language supervision](#). In *International conference on machine learning*, pages 8748–8763. PMLR.
- Alec Radford, Jong Wook Kim, Chris Hallacy, Aditya Ramesh, Gabriel Goh, Sandhini Agarwal, Girish Sastry, Amanda Askell, Pamela Mishkin, Jack Clark, et al. 2021b. [Learning transferable visual models from natural language supervision](#). In *International conference on machine learning*, pages 8748–8763. PMLR.

- Aditya Ramesh, Prafulla Dhariwal, Alex Nichol, Casey Chu, and Mark Chen. 2022. Hierarchical text-conditional image generation with clip latents, 2022. URL <https://arxiv.org/abs/2204.06125>, 7.
- Aditya Ramesh, Mikhail Pavlov, Gabriel Goh, Scott Gray, Chelsea Voss, Alec Radford, Mark Chen, and Ilya Sutskever. 2021. Zero-shot text-to-image generation. In *International Conference on Machine Learning*, pages 8821–8831. PMLR.
- Robin Rombach, Andreas Blattmann, Dominik Lorenz, Patrick Esser, and Björn Ommer. 2022. High-resolution image synthesis with latent diffusion models. In *Proceedings of the IEEE/CVF conference on computer vision and pattern recognition*, pages 10684–10695.
- Christoph Schuhmann, Romain Beaumont, Richard Vencu, Cade Gordon, Ross Wightman, Mehdi Cherti, Theo Coombes, Aarush Katta, Clayton Mullis, Mitchell Wortsman, et al. 2022. Laion-5b: An open large-scale dataset for training next generation image-text models. *Advances in Neural Information Processing Systems*, 35:25278–25294.
- Bin Shan, Weichong Yin, Yu Sun, Hao Tian, Hua Wu, and Haifeng Wang. 2022. Ernie-vil 2.0: Multi-view contrastive learning for image-text pre-training. *arXiv preprint arXiv:2209.15270*.
- Bowen Shi, Peisen Zhao, Zichen Wang, Yuhang Zhang, Yaoming Wang, Jin Li, Wenrui Dai, Junni Zou, Hongkai Xiong, Qi Tian, and Xiaopeng Zhang. 2024. [Umg-clip: A unified multi-granularity vision generalist for open-world understanding](#).
- Amanpreet Singh, Ronghang Hu, Vedanuj Goswami, Guillaume Couairon, Wojciech Galuba, Marcus Rohrbach, and Douwe Kiela. 2022. Flava: A foundational language and vision alignment model. In *Proceedings of the IEEE/CVF Conference on Computer Vision and Pattern Recognition*, pages 15638–15650.
- Quan Sun, Yuxin Fang, Ledell Wu, Xinlong Wang, and Yue Cao. 2023. Eva-clip: Improved training techniques for clip at scale. *arXiv preprint arXiv:2303.15389*.
- Catherine Wah, Steve Branson, Peter Welinder, Pietro Perona, and Serge Belongie. 2011. The caltech-ucsd birds-200-2011 dataset.
- Hongyu Wang, Shuming Ma, Shaohan Huang, Li Dong, Wenhui Wang, Zhiliang Peng, Yu Wu, Payal Bajaj, Saksham Singhal, Alon Benhaim, et al. 2023. Mag-neto: a foundation transformer. In *International Conference on Machine Learning*, pages 36077–36092. PMLR.
- Wenhui Wang, Hangbo Bao, Li Dong, Johan Bjorck, Zhiliang Peng, Qiang Liu, Kriti Aggarwal, Owais Khan Mohammed, Saksham Singhal, Subhojit Som, et al. 2022. Image as a foreign language: Beit pretraining for all vision and vision-language tasks. *arXiv preprint arXiv:2208.10442*.
- Chan Wu, Hanxiao Zhang, Lin Ju, Jinjing Huang, Youshao Xiao, Zhaoxin Huan, Siyuan Li, Fanzhuang Meng, Lei Liang, Xiaolu Zhang, and Jun Zhou. 2023. [Rethinking memory and communication cost for efficient large language model training](#).
- Chunyu Xie, Heng Cai, Jincheng Li, Fanjing Kong, Xiaoyu Wu, Jianfei Song, Henrique Morimitsu, Lin Yao, Dexin Wang, Xiangzheng Zhang, et al. 2023. Ccmb: A large-scale chinese cross-modal benchmark. In *Proceedings of the 31st ACM International Conference on Multimedia*, pages 4219–4227.
- Chunyu Xie, Jincheng Li, Heng Cai, Fanjing Kong, Xiaoyu Wu, Jianfei Song, Henrique Morimitsu, Lin Yao, Dexin Wang, Dawei Leng, et al. 2022. Zero and r2d2: A large-scale chinese cross-modal benchmark and a vision-language framework. *arXiv preprint arXiv:2205.03860*.
- An Yang, Junshu Pan, Junyang Lin, Rui Men, Yichang Zhang, Jingren Zhou, and Chang Zhou. 2022. [Chinese clip: Contrastive vision-language pretraining in chinese](#).
- Lewei Yao, Runhui Huang, Lu Hou, Guansong Lu, Minzhe Niu, Hang Xu, Xiaodan Liang, Zhenguo Li, Xin Jiang, and Chunjing Xu. 2021. Filip: Fine-grained interactive language-image pre-training. *arXiv preprint arXiv:2111.07783*.
- Qinghao Ye, Haiyang Xu, Guohai Xu, Jiabo Ye, Ming Yan, Yiyang Zhou, Junyang Wang, Anwen Hu, Pengcheng Shi, Yaya Shi, et al. 2023. [mplug-owl: Modularization empowers large language models with multimodality](#).
- Yang You, Jing Li, Sashank Reddi, Jonathan Hseu, Sanjiv Kumar, Srinadh Bhojanapalli, Xiaodan Song, James Demmel, Kurt Keutzer, and Cho-Jui Hsieh. 2019. Large batch optimization for deep learning: Training bert in 76 minutes. *arXiv preprint arXiv:1904.00962*.
- Jiahui Yu, Zirui Wang, Vijay Vasudevan, Legg Yeung, Mojtaba Seyedhosseini, and Yonghui Wu. 2022. Coca: Contrastive captioners are image-text foundation models. *arXiv preprint arXiv:2205.01917*.
- Lu Yuan, Dongdong Chen, Yi-Ling Chen, Noel Codella, Xiyang Dai, Jianfeng Gao, Houdong Hu, Xuedong Huang, Boxin Li, Chunyuan Li, et al. 2021. Florence: A new foundation model for computer vision. *arXiv preprint arXiv:2111.11432*.
- Xiaohua Zhai, Xiao Wang, Basil Mustafa, Andreas Steiner, Daniel Keysers, Alexander Kolesnikov, and Lucas Beyer. 2022a. Lit: Zero-shot transfer with locked-image text tuning. In *Proceedings of the IEEE/CVF Conference on Computer Vision and Pattern Recognition*, pages 18123–18133.
- Xiaohua Zhai, Xiao Wang, Basil Mustafa, Andreas Steiner, Daniel Keysers, Alexander Kolesnikov, and Lucas Beyer. 2022b. Lit: Zero-shot transfer with locked-image text tuning. In *Proceedings of the*

Deyao Zhu, Jun Chen, Xiaoqian Shen, Xiang Li, and Mohamed Elhoseiny. 2023. [Minigtpt-4: Enhancing vision-language understanding with advanced large language models.](#)

A Implementation Details

Configurations of our M^2 -Encoders of different sizes are shown in Table 9. We train M^2 -Encoder series with proxy tasks introduced in Section 2.1, all models are trained from scratch on BM-6B and we adopt slightly different training settings optimized across model scales as shown in Table 10.

Models	Encoder			# Params
	Layers	Width	Heads	
M^2 -Encoder-0.4B	12	768	12	402M
M^2 -Encoder-1B	24	1024	16	924M
M^2 -Encoder-10B	24	4096	32	11.2B

Table 9: Architecture configurations.

Hyperparameter	0.4B or 1B / 10B
Image-text data	BM-6B
Proxy loss balance	$\alpha=\beta=0.3$
Learning rate	$2e-4 / 4e-4$
Optimizer	LAMB (You et al., 2019)
Optimizer parameters	$\beta_1, \beta_2, \epsilon = 0.9, 0.98, 1e-6$
Weight decay	0.05
α, β	0.3
Input resolution	224^2
Patch size	16^2
Overall Batch size	131072 / 143360
GBA-ITC Batch size	32768
Samples seen	9B
Numerical Precision	DeepSpeed bf16
ZeRO Optimization	Partial Redundancy Optimizer (PaRO)(Wu et al., 2023)

Table 10: Training settings for M^2 -Encoders of various sizes.

B Fine-grained Benchmark Details

The English portion of our fine-grained benchmark is derived directly from an open-source dataset, while the Chinese part is created through translation. The fine-grained benchmarks are listed in Table 11. For CUB-200-2011 (Wah et al., 2011), Stanford-Dogs (Khosla et al., 2011), and CARS196 (Krause et al., 2013) datasets, we use the images and labels from their respective test sets.

VG-POS and HOI-POS are designed to represent orientation and interaction relationships, respectively, and consist of selected positive examples from the Visual Genome (Krishna et al., 2017) and HOI (Chao et al., 2015) datasets. Both COCO-MCC and COCO-Count are derived from the COCO (Chen et al., 2015) test set, where COCO-MCC is a multiclass classification dataset that includes fine-grained captions describing the classes of objects in each image, and COCO-Count is constructed specifically to assess the counting abilities of vision-language foundation models, with each image’s caption detailing the types and quantities of objects present. The distribution of our constructed fine-grained benchmark is shown in Table 11.

Dataset	# Images	# Texts
CUB-200-2011	5794	200
Stanford-Dogs	8580	120
CARS196	4021	196
COCO-MCC	2222	2222
COCO-COUNT	3240	3238
VG-POS	3000	53806
HOI-POS	520	8593

Table 11: Data distribution of our fine-grained benchmark.

C Distributions of BM-6B data sources.

Most of our collected bilingual image-text pairs are from publicly available sources, here we detail the data sources of our constructed BM-6B in Table 12.

Language	Dataset	Original	Sampled	Remaining	#image-text pairs
English	LAION-EN(Schuhmann et al., 2022)	2.3B	1.9B	82.6%	3.07B
	COYO-700M(Byeon et al., 2022)	700M	435M	62.1%	
	DataComp-1B(Gadre et al., 2023)	1.4B	737M	52.6%	
Chinese	LAION-CN(Schuhmann et al., 2022)	140M	104M	74.3%	3.01B
	Wukong(Gu et al., 2022)	100M	90M	90.0%	
	Taisu(Liu et al., 2022)	166M	94M	56.6%	
	Zero(Xie et al., 2022)	250M	152M	60.8%	
	LAION-EN translated	-	1.9B	-	
	In-house Data	-	668M	-	

Table 12: Distributions of BM-6B data sources.